Chemosphere 246 (2020) 125751

Contents lists available at ScienceDirect

Chemosphere

journal homepage: www.elsevier.com/locate/chemosphere

A novel UASB-MFC dual sensors system for wastewater treatment: On-line sensor recovery and electrode cleaning in the long-term operation

Wenbin Liu [a, b], Guang Yang [c], Hui Jia [a, b], Jie Wang [a, b, *]

[a] State Key Laboratory of Separation Membranes and Membrane Processes, Tianjin Polytechnic University, Tianjin, 300387, China
[b] School of Environmental and Chemical Engineering, Tianjin Polytechnic University, Tianjin, 300387, China
[c] School of Environmental Science and Engineering, Tianjin University, Tianjin, 300072, China

HIGHLIGHTS

- The UASB-MFC coupling system achieved good sensing and treatment performance during the running.
- The precipitation of Ca^{2+} and Mg^{2+} on the cathode surface cause the decline of MFCs performance.
- The dual-sensor system can achieve in-suit voltage recovery and ECS cleaning.

GRAPHICAL ABSTRACT

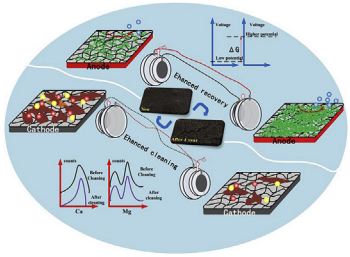

ARTICLE INFO

Article history:
Received 28 September 2019
Received in revised form
24 November 2019
Accepted 24 December 2019
Available online 24 December 2019

Handling Editor: A Adalberto Noyola

Keywords:
Microbial fuel cell (MFC)
Up-flow anaerobic sludge bed (UASB)
Biosensors
Potential distribution recovery
Electrode cleaning

ABSTRACT

In this research, the UASB-MFC dual sensors system was established and treatment the brewery wastewater. The COD removal rate attain about 90% and the NH_4^+-N concentration less than 15 mg/L, MFCs has a voltage range of 0.34–0.42 V. Meanwhile, as the biosensor for coupling system, MFCs can be used to make simultaneous monitor COD and TVFA. The potential distribution can in-situ accelerate the reattachment of micro-organisms, which shorten the recovery time to 55% of the original. The long-term performance of MFCs were tested by electrochemical methods and found that the degradation of biosensors was mainly caused by the precipitation of Ca^{2+} and Mg^{2+} on the cathode surface and affected by concentration. More importantly, cleaning the electrode by an self-enhanced method without external assistance ECS (Electrodes Connection Switching) can improve the MFCs performance to 83.2 %–84.6%. Dual sensors system in UASB gives a novel possibility for UASB-MFC sensor self-sustaining in a long-term.

1. Introduction

Microbial fuel cells (MFCs) are consist of anode and cathode, which separated by an ionic exchange membrane in traditional systems (Velasquez-Orta et al., 2017; Palaniappan et al., 2019). However, the use of exchange membrane increases the running cost, more and more scholars began to study the non-membrane MFC. It was found that the non-membrane structure would not affect the electricity production of MFC (Feng et al., 2015; Soon et al., 2015; Liu and Logan, 2004). MFC is a technology based on microbial, which can convert organic to produce electricity by

* Corresponding author. State Key Laboratory of Separation Membranes and Membrane Processes, Tianjin Polytechnic University, Tianjin, 300387, China.
E-mail addresses: wangjiemailbox@163.com, wangjie@tjpu.edu.cn (J. Wang).

https://doi.org/10.1016/j.chemosphere.2019.125751
0045-6535/

microbial degradation (Logan et al., 2006). The characteristic of electricity production and simultaneous wastewater treatment for MFCs has drawn much research attention recently (Pandey et al., 2016; Liao et al., 2015; Wang et al., 2018). For example, Tejedor-Sanz et al. (2017) developed a merging microbial electrochemical system and with electrocoagulation as pretreatment, achieving a complete treatment of brewery wastewater. Ray and Ghangrekar (2015) developed a coupling system to enhance the organic matter removal, biopolymer recovery and electricity generation from distillery wastewater by combining fungal fermentation and MFC. A wide variety of MFC coupling systems make it widely used in the field of wastewater treatment (Tian et al., 2015; Li et al., 2016; Zhang et al., 2019; Liu et al., 2018; Yang et al., 2019). Moreover, as electro-active microorganisms in the anode are able to degrade organic matter, the magnitude of electrical current generation has been proven to be related to the organic matter content in wastewater (Yang et al., 2015). Such as Chen et al. (2016) developed a novel biosensor for P-nitro phenol based on MFC. Zeng et al. (2017) developed a single chamber air-cathode MFC for online monitoring levofloxacin. Recently, Jia et al. (2017, 2018) constructed a UASB-MFC integrated system, enhancing simultaneous response and amplification of the MFC-based biosensor by adding zero valent iron. However, using one MFC as the biosensor for the coupling system has some limitations, such as less feedback information, lack data stability, and poor performance and so on. Most importantly, it is difficult to solve the problems of long restart up time of the MFC-based biosensor after affected by adverse environment and the degradation of MFC performance during the long-term operation (Elmekawy et al., 2018).

The most valuable features of MFC-based biosensors were its self-sustaining, no external power sources and without additional signal transducer (Stein et al., 2011; Wang et al., 2019; Jiang et al., 2018). But the degradation of bio-electrode activity greatly limited the advantages. Based on the previous study, the UASB-MFC dual sensors system was constructed in this research, using two different MFC as the biosensors for coupling system and on-line monitoring the operating conditions of the UASB reactor. Which can not only achieve a wide range of in-suit monitoring, but also improve the ability to conduct a more comprehensive evaluation of the operation about the system. Meanwhile, the potential distribution in the dual sensors system made it possible to balance the electrode properties after affected by adverse environment. The performance of the MFCs during the long-term operation were tested by electrochemical methods, and the advancement of electrochemical tools used in this study enables direct characterizations of electro-active biofilm activities and catalyst performance under changing environmental (He and Mansfeld, 2009). Moreover, some investigations for electrode cleaning including on-line ECS cleaning and AC enhanced were carried out, which expect to improve the long-term performance of MFCs.

2. Materials and methods

2.1. Integrated system

The UASB-MFC coupling system consists of a UASB reactor and two bio-cathode MFCs without proton exchange membrane (PEM) (Fig. S1). The whole device was constructed from transparent polyvinyl chloride (PVC) tube with a total volume of 2.5 L (150 cm long by 8 cm diameter), and the working anaerobic sludge volume in the reactor lasted 1.2 L. In order to maintain a constant biomass, which was regularly measured and properly discharged during the operation. The inoculated sludge was taken from the secondary settling tank of Municipal Sewage Treatment plant (Tianjin, China). Cleaning removes impurities and the sludge concentration was 6200 mg/L. After 60 days of adaptation and then added to the UASB reactor. The influent at the lower end was provided with a water tank through a peristaltic pump (KSN-203, Kosuno, Guangdong Shantou Kosuno Limited by Share Ltd). A flow meter (LMF-1, Changchun Lvqingqi Co., Ltd., China) was connected to the gas outlet of the three-phase separator in the UASB, Hydraulic retention time (HRT) lasted 12 h, with the flow rate being 0.058 mL/s. Respectively, coupling MFCs were in sludge layer (0.35 m) and suspended layer (0.85 m) of UASB reactor. The MFCs anodes are placed directly inside the UASB reactor, and the cathodes are located outside the protruding pole chamber. The integrated system was pretreated by biogas, and it was operate in continuous mode at room temperature (22 ± 1 °C).

The air-cathode MFC was constructed as previously described (Kim et al., 2015), which is a cylindrical chamber and the effective volume is about 120 mL. The MFC anode material is carbon felt (Diameter 5 cm; PAN, Beijing Peak Xiang Co.), the cathode material is carbon cloth (8 × 6 cm; HCP330, Shanghai Hesen Electric Co Ltd), and 3 cm distance between anode and cathode. The electrode material was prepared according to the previously described (Zhang et al., 2010). The electrical circuit connected between anode and cathode was fabricated by copper wires with a resistance of 1000 Ω, and the voltage across resistor was collected every 30 min by a data acquisition instrument (34972 A, Keysight, USA), in the middle position of the anode and cathode insert Ag/Agcl (+0.21 V versus standard hydrogen electrode, 25 °C) reference electrode.

2.2. Composition of the wastewater

The wastewater treatment by UASB reactor is brewery wastewater and which taken from the winemaking process and the properties are shown in Table S1. The wastewater was continuous delivered to the UASB-MFC coupling system with a peristaltic pump, which enters the reactor from the bottom and decomposed by anaerobic sludge at reaction zone, and then the effluent discharged from top of the reactor.

2.3. Analytical and connection methods

The concentration of COD, NH_4^+-N, and TP were analyzed by a HACH DR/2400 Spectrophotometer (HACH Company, USA) according to the standard operating procedures. VFAs were determined using GC (GC-2014, Shimadzu, Japan) with a flame ionization detector and capillary column (Stabil wax-DA, 30 m × 0.25 mm × 0.25 μm). The flow rate and the temperature of the column were maintained at 0.6 mL/min and 230 °C respectively, and other programs followed by previous methods (Jiang et al., 2014). Biogas generated from the reactor was measured by wet gas flow meter and analyzed for methane composition using Gas Chromatography (GC-2010, Shimadzu, Japan).

To characterize the detailed morphology of the samples, field-emission scanning electron microscopy (FE-SEM) (Hitachi S-4800, Japan) was used. Chemical compositions of the catalyst layer were analyzed using X-ray photoelectron spectroscopy (XPS, ESCALAB 250Xi, Thermo Fisher) (Deng et al., 2017). The changes of the bacterial in biofilm were fluorescent staining using a LIVE/DEAD Backlight Bacterial Viability Kit (L7007, Thermo Fisher Scientific Inc., USA) (Ren et al., 2011).

The dual sensors system has the ability of in-situ recovery and self-enhanced electrode cleaning. To accelerate the recovery of MFC, connect the same electrodes of two sensors to each other (MFC recovery means that when the MFC inhibited by the adverse environment and voltage decreased rapidly, the electrode potential was improved by some methods to accelerate the microorganisms reattachment, which eventually makes the voltage of MFC quickly

restored to normal state). When the electrode needs to be cleaned, the electrodes of two sensors are alternately connected positively and inversely every 15 min (Electrode cleaning is a necessary process to maintain MFC sensors stable state, improve the electricity production performance of MFC, which can clean the biofilm and precipitation ions attached to the surface of the cathode by alternating current). The detailed connection information you can get from Fig. S2.

2.4. Electrochemical tests

MFCs were characterized using several electrochemical techniques with a potentiostat (PC4/750, Gamry Instruments): linear sweep voltammetry (LSV), cyclic voltammetry (CV), potentiostatic polarization, galvanostatic polarization, and electrochemical impedance spectroscopy (EIS). LSV was carried out with the three-electrode system. EIS was used to analyze internal resistance of MFC, which mainly included the charge transfer resistance of bio-anode, the solution and diffusion resistance. Impedance measurements were conducted at the open circuit potentials with the voltage amplitude of 10 mV over the frequency range from 10,000 Hz−0.1 Hz (Wu et al., 2016).

The external AC currents (Model 188-s-1257, Wavetek Co., CA, USA) were applied to the MFCs after a long-term operation. Two-electrode system with 1 Hz frequency and 20 V amplitude was used in the testing process. Respectively connect working electrode and opposite electrode separately, cleaning for 45 min. The electrochemical performances of MFCs were retested after 24 h at the end of the cleaning.

Current (I) was calculated at a resistance (R) from the voltage (V) by $I = V/R$. Power (P) was calculated $P = I \times V$ and normalized based on cathode projected surface area.

3. Results and discussion

3.1. Long-term performance

MFC as the biosensor for the coupling system can be used to monitor the operating state of UASB reactor, which can regulate the operation parameters and improve the stability of anaerobic reaction by using an electrical signal (Jia et al., 2018). Therefore, the performance of the biosensors become the key to wide applications for UASB-MFC coupling system. Fig. 1a described the voltage changes of MFCs during the long-term operation in this work. It is worth noting that the voltage of MFCs decreases with operation time and the drop were about 0.03 ± 0.005 V, which indicated that the performance of MFCs decreased after running. Moreover, MFCs appeared some recoverable drop points during the long-term operation, which could be due to the massive accumulation of volatile fatty acids (VFAs) in short-term or other adverse environmental conditions, resulting in the inhibition of bacteria activity and spalling from the anode surface. Fortunately, the bacteria activities can self-recovery and make the voltage attained to the normal state by optimum the operating conditions.

To make full use of the simple feedback electrical signals of the MFC-based biosensor to on-line monitoring the operator state of the UASB reactor, the relationship between MFCs voltage and COD or TVFA concentrations were established (Fig. 1b), it was found that the fitting curve has good relevance. However, the long-term error value record showed that the error of feedback information increased with the extension of running time. Whatever the concentration error and voltage error, the larger of $MFC_{sludge\ layer}$ with the running, which contribute to the higher sludge concentration and rapid degradation of MFC electrode (Fig. 1c). The error value represents the difference between the true value and the fitting curve value, which indicates the relevance of feedback signals. The greater the error value, the more deviant of the feedback is. The above results further explain the weakening of the biosensor during the long-term operation (Zhao and Kong, 2018).

In addition to the MFC sensing effect, the treatment efficiency of the coupling system is also the key to wastewater treatment. Therefore, the relevant chemical indicators about the treatment efficiency were tested during the long-term operation. The effluent COD is an important index for brewery wastewater standard discharge, a good treatment efficiency achieved after continuously running for 60 days, which the removal rate of COD can reach about 90% (Fig. S3a). Meanwhile, the NH_3−N and TP showed the same trend, and the concentration of NH_3−N, TP was less than15 mg/L, 2 mg/L (Fig. S3b). In UASB-MFC coupling system, the wastewater treatment was an anaerobic digestion process. The most of the organic matters decomposed by anaerobic sludge and discharged biogases, such as methane (CH_4), carbon dioxide (CO_2) and oxygen (O_2) (Kang et al., 2018). Therefore, the total gas production and the proportion can evaluate the anaerobic digestion process to some extent (Zhang et al., 2015). During the stable operation state, the biogas production is about 600 mL/d, which the methane was the main component and accounting for about 62% of the total gas output (Fig. S3c). Volatile fatty acids (VFAs) are important intermediate by-products in anaerobic digestion to produce methane, and its concentration can indicate the equilibrium state of anaerobic reaction (Huang et al., 2015). Except for the VFAs concentration, the composition and proportion of VFAs also affect the performance of anaerobic sludge (Miao et al., 2013; Wagner et al., 2014). In Fig. S3d, VFAs mainly include acetic acid, propionic acid, butyric acid. It can be seen that the accumulation of VFAs reached a stable level at the 90th day of operation and is about 200 mg/L, the acetic acid (HAC) concentration was maintained at about 150 mg/L and as much as 75%, which basically reached the required level of effluent from the anaerobic reaction that had been reported before to run well (Lee et al., 2014).

Based on the more than one year running, the results showed that MFC-based biosensors could monitor the UASB running states on-line by voltage signals, which given more valuable information for UASB operating. However, in view of the long-term running of MFCs, the deactivations of electrodes have been largely limited the MFC-based biosensors. It is necessary to do more in-depth researches and find effective solutions to maintain the sensing activities of MFC-based biosensors.

3.2. Recovery of MFC biosensors

Good recoverability was necessary if the biosensor could be applied for a long time (Jiang et al., 2017). The recovery time is too long about the MFC-based biosensors also exist in the UASB-MFC dual sensors system (Kaur et al., 2014). Due to the high substrate concentration or short hydraulic retention time (HRT), the anaerobic equilibrium would be destroyed. The rapidly accumulation of VFAs cause the decrease of pH, which resulted the severe scenario and inhibits the metabolism activity of microbial (Rebecchi et al., 2016). It is well known that the exoelectrogens play the key role in MFC-based biosensor, which attach to the anode surface to decompose organic matter and convert it to electrical signals. Exoelectrogens are widely distributed in all kinds of microbial flora, and mainly by the *Geobacter, Shewanella, Pseudomonas* and other metal dissimilation bacteria (Pandey et al., 2016). The accumulation of VFAs cause the decrease of pH in the system, which have a strong inhibitory effect on these bacteria (Kaur et al., 2013). Therefore, the excessive VFAs caused by the poor performance of the system and resulted in the inhibition of microbial growth, which cause a large number of microbes to die and fall off from the anode surface, lead

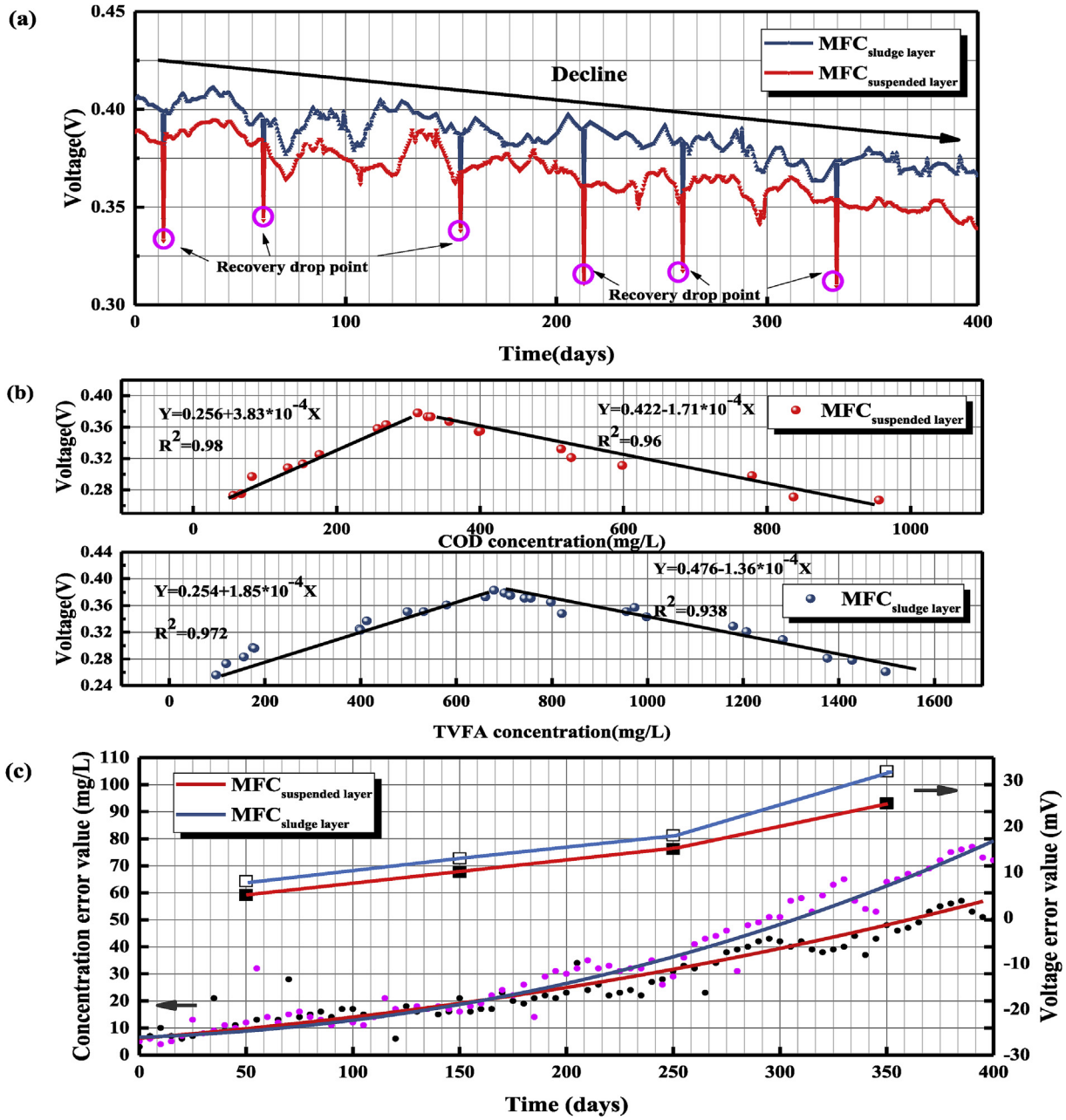

Fig. 1. The long-term performance of MFCs. (a) the voltage output of MFCs. (b) the fitting curves of MFCs. (c) the error value of fitting curves.

to the MFC voltage of greatly reduced. But owing to the microbes self-reproduction, which can improve the microbial growth environment and make the microbes reattached to the anode surface by adjusting the external system parameters. Therefore, the voltage recovery of the MFC-based biosensor can be regard as the microbial reattachment on the anode surface. In order to shorten the recovery time of MFC, it is necessary to accelerate the microbial enrichment on the anode surface.

During the long-term operation of the UASB-MFC dual sensors system, it was found that MFCs have good recovery ability (Fig. 2a). However, it worth noting that the recovery time of the $MFC_{suspended\ layer}$ was longer after inhibited by the adverse environment (Fig. 2a). This probably caused by the $MFC_{suspended\ layer}$ anode was located in the suspended layer of the UASB reactor, and the small amount of micro-organisms has poor self-repair ability. In order to solve the problem of long recovery time of the $MFC_{suspended\ layer}$, this work used the unique advantage of the dual sensors system in structure to improve the anode potential and accelerated the voltage recovery by in-situ potential distribution. Due to the different sludge concentrations in suspended layer and sludge layer of the UASB reactor, there were some differences in voltage about MFCs and the $MFC_{sludge\ layer}$ potential was higher, which made the paralleled $MFC_{suspended\ layer}$ under the higher potential recovery conditions. On the one hand, the higher potential caused the substrate driving force of exoelectrogens catalytic oxidation increased and promoted the growth of exoelectrogens on the anode surface. On the other hand, the higher the anode potential, the more energy the bacterium got and accelerated the electron transfer process (Finkelstein et al., 2006; Wang et al., 2009). In Fig. 2, it can be seen that the self-recovery time of MFCs after inhibited by adverse environment is

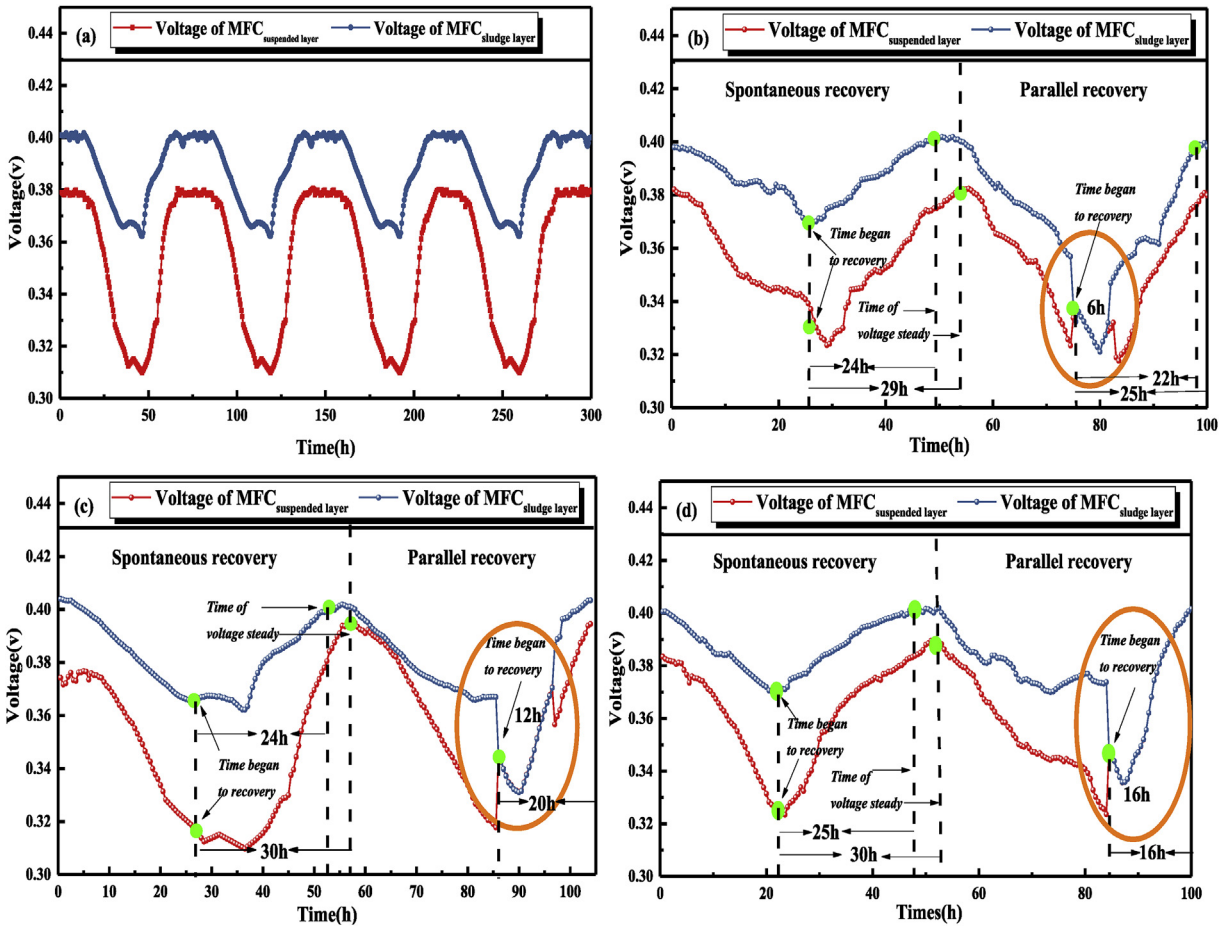

Fig. 2. Repeatability and recoverability of MFCs. (a) Repeatability of MFCs. (b) Recovery time of parallel 6 h. (c) Recovery time of parallel 12 h. (d) Recovery time of parallel 16 h.

about 24–25 h ($MFC_{suspended\ layer}$), 29–30 h ($MFC_{sludge\ layer}$), respectively. When the MFC-based biosensor was inhibited by severe conditions, the external parameters could be adapted to recover, and the method was to connect the same electrode of MFCs to form a parallel system. When the connection had lasted for 6 h, the final recovery time of $MFC_{suspended\ layer}$ was shortened to 25 h, and the $MFC_{sludge\ layer}$ was shortened to 22 h (Fig. 2b). After 12 h of parallel connection, the final recovery time of MFCs were shortened to 20 h (Fig. 2c). Similarly, after 16 h of parallel connection, the MFCs have been fully recovered (Fig. 2d). On the whole, it is demonstrated that the effect of potential distribution on accelerating the recovery of the $MFC_{suspended\ layer}$ is more obviously (Table S2), which is owing to the potential of $MFC_{suspended\ layer}$ was promoted higher. The higher the current is, the more intense of the redox reaction on the electrode surface, which accelerates the electron transfer process (Gupta et al., 2017). Moreover, the higher potential enhanced the substrate driving force and metabolic activity of the exoelectrogens, and made them become the dominant population in the process of competition. The competitiveness of other bacteria on the electrode surface gradually weakened and then dropped from the electrode. Therefore, the resistance of electrons in the transmission process was reduced. Meanwhile, the recovery time of $MFC_{sludge\ layer}$ had also been slightly shortened in the process of cooperative recovery, which possibility that the $MFC_{suspended\ layer}$ may also play a supplementary part at some point. In order to better understand the effect of higher potential on accelerate of MFCs recovery, the recovery time was compared between the traditional applied electric field method and the in-situ recovery method. From Table S3, it is clearly seen that the reduction of recovery time is more obvious by the method of applied an electric field and the magnitude of additional electric field has little effect on the recovery time. However, the methods of additional electric field need more auxiliary equipment, which increase the cost and difficulty of using MFC-based biosensor. Therefore, the in-situ recovery of the dual sensors system is more practical by cost saving.

In order to comprehensive evaluate the impact of potential distribution on MFCs voltage recovery, the electrochemical tests were carried out at the same time. Fig. S4a described the impedance of the $MFC_{suspended\ layer}$ under different conditions. The diameters of the semicircle corresponds to the interfacial charge-transfer resistance (Rct), which usually represent the resistance of electrochemical reactions on the electrode and are called the Faraday resistance, the smaller the radius, the less the resistance would achieve (Bard and Faulkner, 2001). It can be seen from Fig. S4a that the impedance radius is decreasing with the extension of parallel time. When the parallel time is 16 h, the impedance radius is the same as stable scenario, which indicated that the $MFC_{suspended\ layer}$ attained normal conditions. In the same recovery time, the impedance radius (black line) of the $MFC_{suspended\ layer}$ under high potential (HPOT) is smaller than that of natural state (grey line), which further shows that the HPOT reduced the resistance of electron transfer and accelerate the redox reaction. Meanwhile, from the voltage-time and potential-time curves, it can be seen that the longer the parallel time is, the more obvious the acceleration of $MFC_{suspended\ layer}$ recovery is (Fig. S4b, Fig. S4e). CV

curve can directly characterize the microbial activity on the anode surface, which results also confirm that HPOT enhance the activity of biofilm (Fig. S4c). In order to evaluate the performance of $MFC_{suspended\ layer}$ more comprehensively, the maximum power density of $MFC_{suspended\ layer}$ was measured synchronously. From Fig. S4d, it can be seen that in the same recovery time, the maximum power density under HPOT recovery conditions is higher than that of self-recovery. Moreover, the maximum power density is increasing with the extension of HPOT connection. The above results confirms that the effect of higher potential accelerate the recovery is more obvious with the prolonging of time, and the biosensor can be completely restored to its original stable state when the HPOT connection lasted for 16 h.

The surface changes of the MFC electrode can be directly demonstrated by electrochemical method. In order to further prove HPOT accelerating the MFC recovery and more intuitively reflecting the microbial enrichment on the anode surface, the biomass on anode surface under different conditions were analyzed by laser confocal method (Fig. S5). It can be clearly seen that the density of green dots increases with time, regardless of self-recovery conditions (Figs. S5a–c) or HPOT-recovery conditions (Figs. S5d–e). It shows that the amount of microbial adhere to the anode surface is increasing gradually. However, the density of green dots in self-recovery conditions (Fig. S5c) were less than that in HPOT-recovery conditions. This is owing to the higher potential gives negative charge micro-organisms the power to preferentially adsorb on the electrode surface (Fig. S5f). The start-up of MFC is closely related to the growth of exoelectrogens on the anode surface, and the more biomass attached to the electrode surface at the same time, the shorter the starting period was (Paitiera et al., 2017; Hong et al., 2011; Cheng et al., 2011; Zhou et al., 2020). Therefore, the above results further confirm that the HPOT can accelerate the process of biofilm adhesion to the anode surface and shorten the recovery time of MFC.

The problem of the long recovery time of MFC in UASB-MFC dual sensors system was effectively solved by using the in-situ recovery. The coupling system not only can make the anaerobic reactor keep a longer stable running period, but also expands the application of MFC-based biosensor by the structure and self-regulation optimization.

3.3. Electrodes degradation and cleaning

In this work, the UASB-MFC coupling system was running at continuous mode for more than one year to examine the MFC-based biosensors long-term performance. In order to insight the performance of MFCs, the electrochemical tests were carried out during the long-term operating process. Fig. 3 is the changes of electrode potential of the MFCs during the long-term operation. The curves of the electrode potentials against current density were used to evaluate the performance of electrodes. For a fixed current density, the higher the potential, the better the performance of the electrode is obtained (Cheng et al., 2006).

In Fig. 3, the electrode potential measured at different time which shows the same trend, and this indicated that the electronic transfer mechanism of MFCs is the same in a long run. The anode potential can directly characterize the activity of the anode biofilm. In Fig. 3 (a, b), it can be seen that the anode potential fluctuates to a certain extent during the long and stable operation, but the overall changes are not significant (±0.02 V). In contrast, the fluctuations of cathode potential are larger, C_i-C_0 represents the difference value between the different stages potential and the initial potential of the electrode. It can be seen from Fig. 3 (c, d), the C_i-C_0 (−0.20-0 V) are all negative and the absolute value of C_i-C_0 is increasing ($C_3-C_0 < C_2-C_0 < C_1-C_0$). The above results indicate that the degradation of the cathode is more obvious, which was mainly contribute to the degradation of MFCs performance.

In order to further understand the mechanism for the degradation of cathode performance of the MFCs, a series of studies on cathode materials and surface appendages were carried out. Firstly, the surface of the electrode (Fig. 4 a-c), the surface of the catalyst (Fig. 4 d-f), and the surface of the carbon cloth were all analyzed by FESEM (Fig. 4 g-i). It can be seen from Fig. 4a that the surface of the new electrode is more smooth and cleaner than used one (Fig. 4b). After a long period of operation, a layer of biofilm attached to the electrode surface which play an important role in bioelectricity generation (Fig. 4b), but undesired biofilm layer growth may cause a variety of problems such as biofouling, microbial influenced corrosion, infection, and contamination (Miller et al., 2012). The complicated deposition on the cathode surface, hinder the proton transfer, reduces the diffusion rate of oxygen to the anode, which lead to the decrease of power density. After scanning surface layer, the catalyst layer was also scanned again and found that the catalyst layer surface was smooth before using (Fig. 4d). In contrast, there were massive white crystals attached to the surface of catalyst layer after used (Fig. 4e), and preliminary speculations were metal deposits under the action of the internal electric field. In order to prove this point of view, the elemental analyses were carried out before and after the using (Fig. S6). According to Fig. S6 (d. e) and Table S4, Ca^{2+} and Mg^{2+} give important contribution to the phenomenon. The content of Ca^{2+} and Mg^{2+} on the electrode surface increased greatly after the long-term running, which further proved that the occurrence of salting out phenomenon. Due to the existence of electron transfer process in MFC, a weak electric field will be formed between the anode and the cathode. Under the electric field force, the positively charged Ca^{2+} and Mg^{2+} will move towards to the cathode and accumulate on the electrode surface. Ultimately, the Ca^{2+} and Mg^{2+} adhere to the cathode surface in the form of precipitation. However, the deposition of Ca^{2+} and Mg^{2+} covered the active site of the catalyst surface, which reduced the activity of the catalyst to a certain extent. The analysis of the carbon cloth surface showed that there were also a small amount of Ca^{2+} and Mg^{2+} attached to the carbon cloth gap, which blocked the micro pores of the material surface and decreased the efficiency of the air diffusion. Meanwhile, the maximum power density and internal resistances of MFCs were measured (Fig. 6). The initial maximum power density of $MFC_{suspended\ layer}$ is 0.143 ± 0.002 W/m^2, and $MFC_{sludge\ layer}$ is 0.176 ± 0.002 W/m^2, respectively (Fig. 6a). The difference in the maximum power density of MFCs was mainly caused by the different microbe's concentrations of suspended layer and sludge layer in UASB reactor. Similarly, the maximum power density of MFCs decreased about 0.02 ± 0.002 W/m^2 after 6 months of operation. After one year of operation, the MFCs maximum power density were reduced to 0.109 ± 0.002 W/m^2 ($MFC_{suspended\ layer}$, 76.2 ± 0.2% of the initial state), 0.136 W/m^2 ($MFC_{sludge\ layer}$, 77.2 ± 0.2% of the initial state), respectively (Fig. 6a). Meanwhile, it can be seen that the impedance during the long-term operation is increasing (Fig. 6b), which indicates that the inhibition effect of the surface electrons in the transmission process got stronger. Therefore, the electron transfer efficiency was reduced and the performances of MFCs are influenced. The above results demonstrated that power density decreased and resistance increased with Pt-catalyzed air-cathode after long run.

The key to prolong the life cycle of the MFC-based biosensor is to find out the factors that affect the degradation of the electrode. Therefore, it is necessary to study whether the concentration of Ca^{2+} and Mg^{2+} in brewery wastewater have an effect on the degradation of MFC sensors or not. The changes of maximum power density of MFCs were tested under different concentrations of Ca^{2+} and Mg^{2+} in brewery wastewater by comparison experiment.

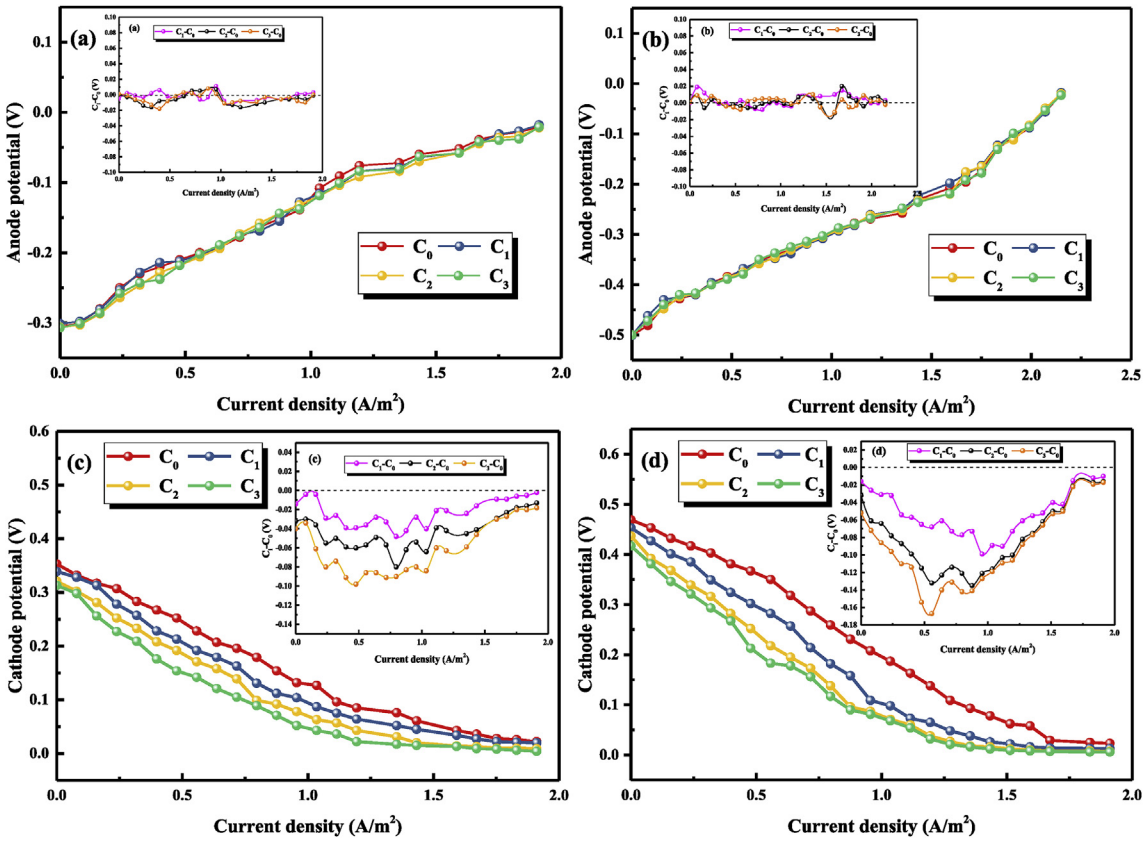

Fig. 3. The long-term performance about anode and cathode potentials of MFCs (C_0-1Day, C_1-3months, C_2-6months, C_3-12months). (a) The anode potenials of $MFC_{suspended\ layer}$. (b) The cathode potenials of $MFC_{suspended\ layer}$. (c) The anode potenials of $MFC_{sludge\ layer}$. (d) The cathode potenials of $MFC_{sludge\ layer}$.

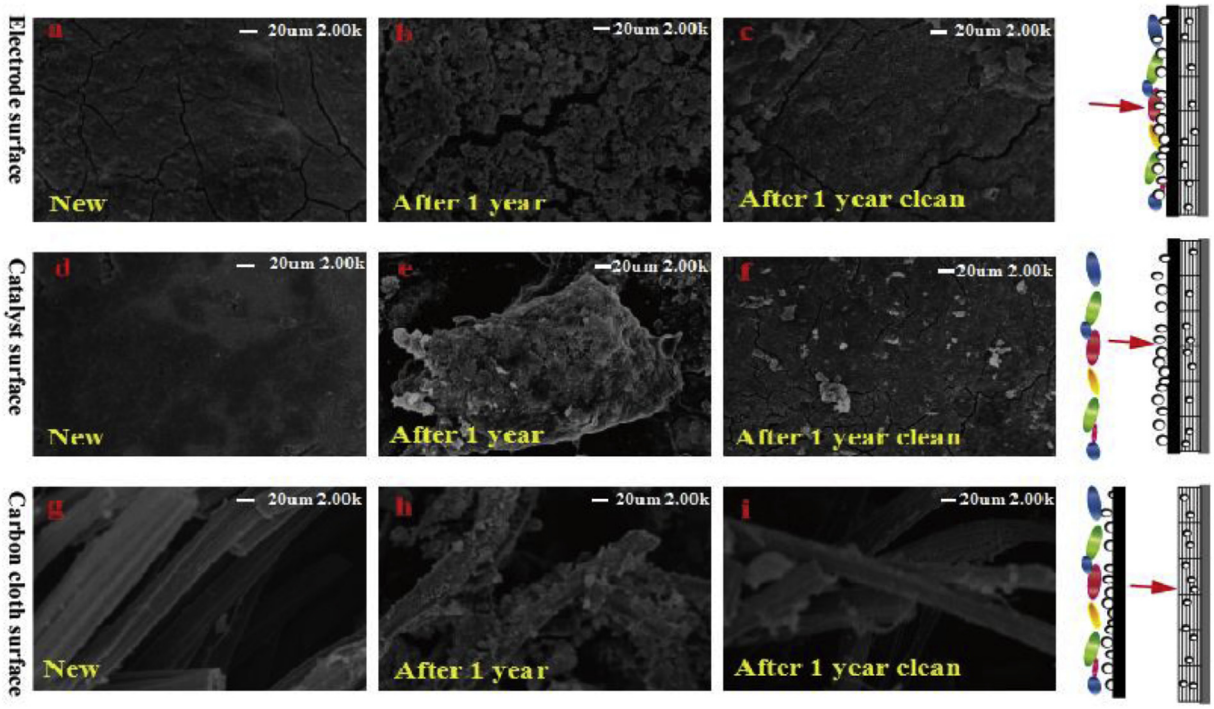

Fig. 4. FESEM images on cathode carbon cloth. (a–c) Electrode surface new and after 1 year. (d–f) Catalyst surface new and after 1 year. (g–i) Carbon cloth surface new and after 1 year.

It can be seen from Table S5 that the increase of ion concentration can enhance the electron transfer rate and increase the maximum power density of MFCs, but the higher the concentration of Ca^{2+} and Mg^{2+}, the more obvious the degradation of MFCs performance with the prolong of running. Therefore, in order to better mitigation the degradation of MFC performance, the concentration of Ca^{2+} and Mg^{2+} should be controlled by pretreatment. Certainly, properly reduced the electrode potential is more conducive to prolong the use of MFC-based biosensor. Most importantly, in order to keep good performance of MFC-based biosensor in long-term operation and mitigation the degradation of the electrode, it is necessary to take some methods to clean the electrode. Previous studies have shown that super high voltage, such as 13–35 kV amplitude, and low-frequency AC (5–15 V amplitude, 1–10 Hz) can kill bacteria because super high voltage AC provides a strong electric field force (Chen et al., 2008; Hoseinzadeh et al., 2018). In the UASB-MFC dual sensors system, due to the MFCs in different sludge concentrations positions, which cause a potential difference between the two biosensors. Therefore, the ECS method was propose to clean electrodes in this work (Fig. S2). The cathode can be cleaned by the positive and negative connection of MFCs electrode in-situ. In order to found out the best cleaning parameters of ECS method, the cleaning effect were compared under different electrode alternating interval and cleaning time. It can be clearly seen from Fig. 5 (a,b), the performance of MFC improves rapidly and then steadily with the prolong of cleaning time under the same electrode alternating interval, and the cleaning effect is the best when the ECS cleaning lasted 3 h. Similarly, the electrode alternating interval also play a key role on the effect under the same cleaning time, and 15 min is the most effective (Fig. 5a and b). Meanwhile, the voltage of MFC were measured under different ECS cleaning within 400–450 day, which can more directly reflect the change of MFC performance. Fig. 5 (c,d) demonstrated that the MFC voltage decreases with the extension of running time, but the voltage decline alleviated under different ECS cleaning (every ten days was chosen as a cleaning cycle). The effects of electrode alternation interval and cleaning time on ECS method need to be further studied. According to the above results, connecting the two sensors anode and cathode alternately at intervals of 15 min, continuous cleaning 3 h and then disconnected 24 h for MFCs recovery. After a series of cleaning, the microbes on the electrode surface were abscised partly (Fig. 4c). The white crystal on the surface of the catalyst and the comminuted crystal of the carbon cloth crevice were also shredded obviously (Fig. 4f, i), and the XPS tested also showed that after the in-situ ECS cleaning the content of Ca^{2+} and Mg^{2+} decreased (Fig. S6 d,e and Table S4). The performance of MFCs were measured by electrochemical method and found that the $MFC_{suspended\ layer}$ maximum power density increased from 0.106 ± 0.01 W/m^2 to 0.119 ± 0.01 W/

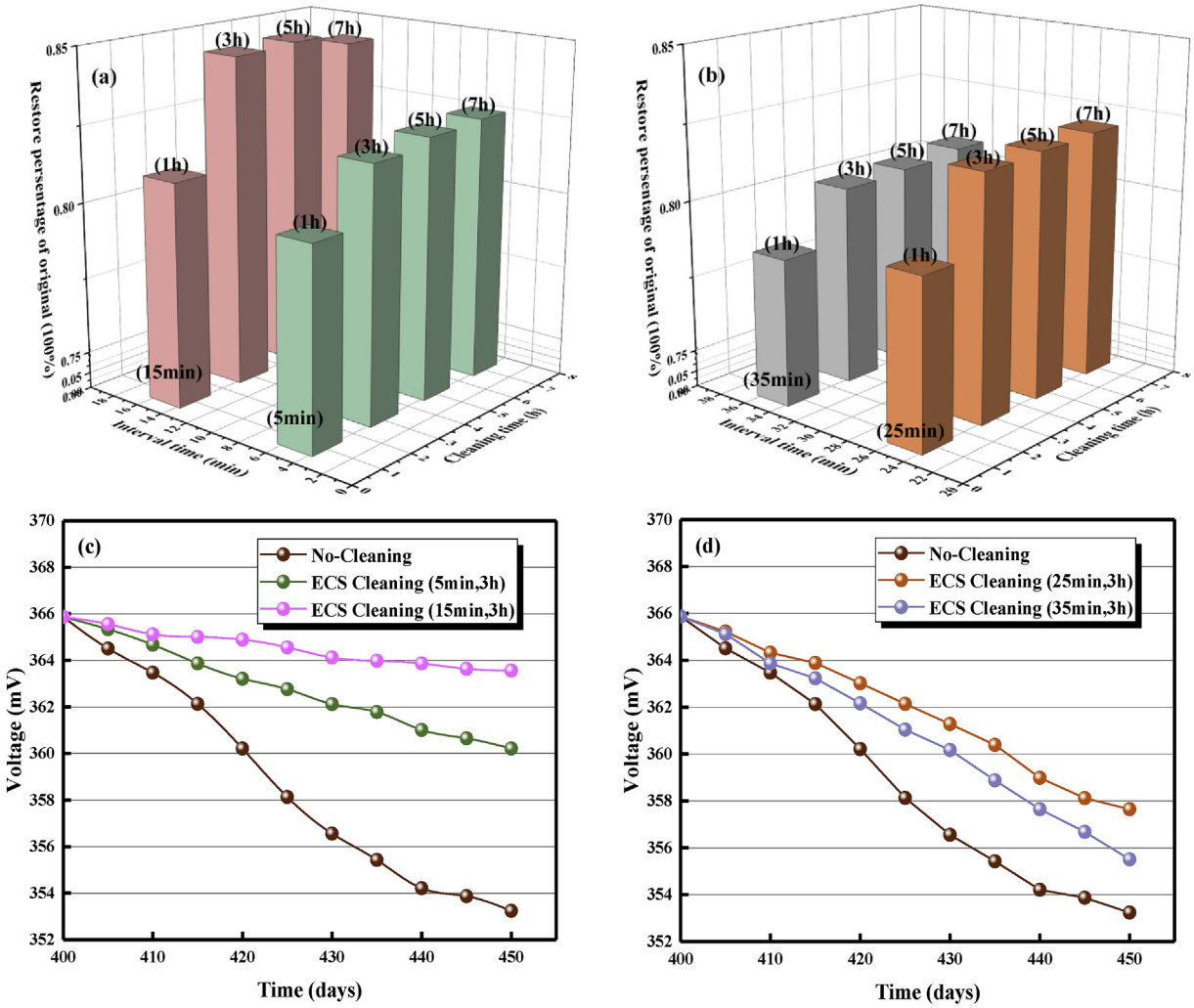

Fig. 5. The ECS cleaning effect and MFC voltage under different electrode alternating interval and cleaning times. (a,b) ECS cleaning effect under different electrode alternating interval and cleaning time. (c,d) MFC voltage under different ECS cleaning.

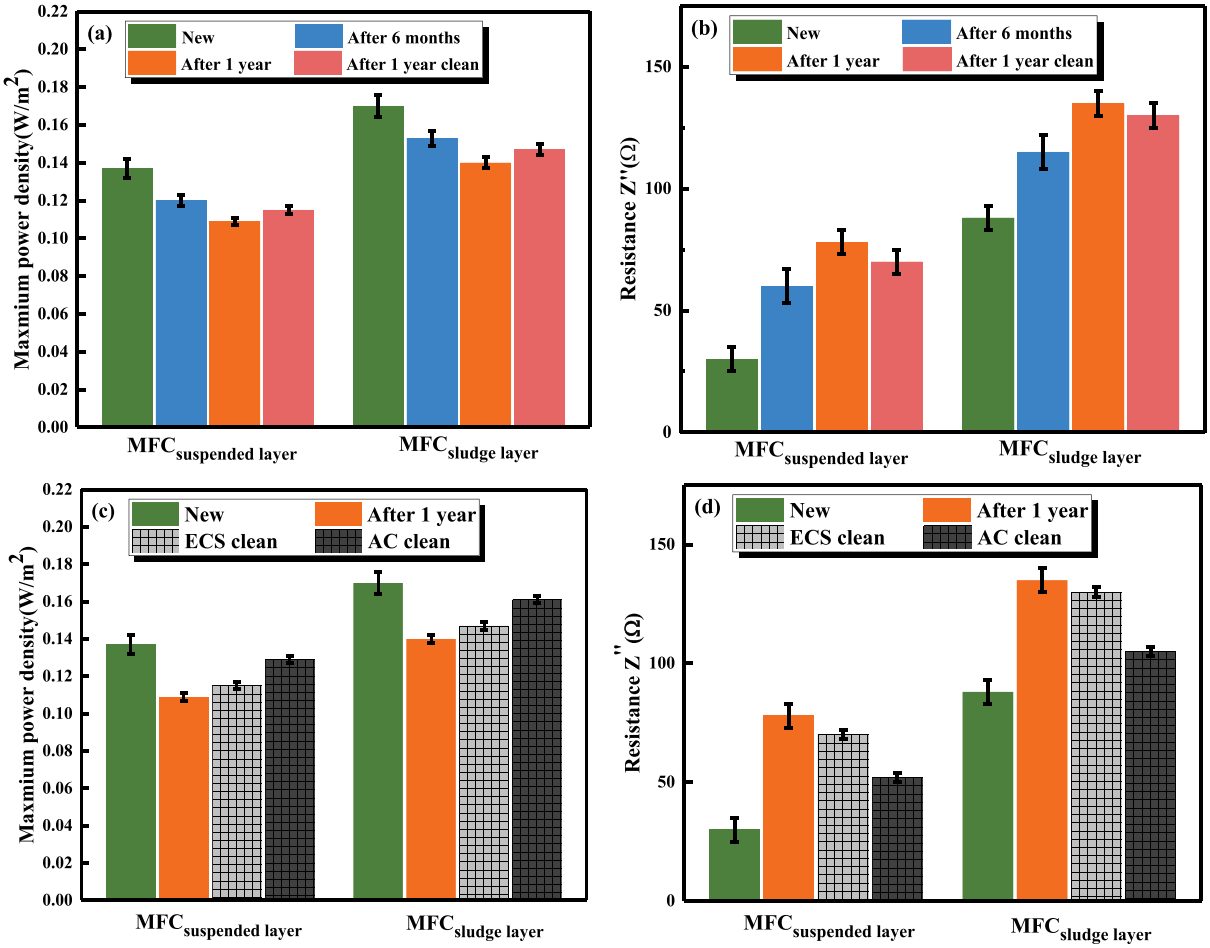

Fig. 6. The long-term Maximum power density and Resistence of MFCs. (a) The Maximum power density of MFCs. (b) The resistance of MFCs. (c) The different cleaning effect about Maximum power density. (d) The different cleaning effect about resistance.

m^2 (increased to 83.2 ± 0.02% of the original), and the $MFC_{sludge\ layer}$ increased from 0.136 ± 0.01 W/m^2 to 0.149 ± 0.01 W/m^2 (increased to 84.6 ± 0.02% of the original) (Fig. 6a), the impedance of the MFCs were reduced by about 13.8 %–18.7% (Fig. 6b). The above results show that in-situ ECS cleaning can mitigation the decline of the MFC performance, this is because the biofilm was damaged and make the intercellular electron transfer network loss by electro-hydrodynamic force. Moreover, the lower frequency AC current led to water electrolysis, which generated gas bubbles that flushed all attached cells out of the electrode. In order to further enhance the cleaning effect, the cathodes were cleaned by external AC in this work. The working electrode and the opposite electrode of the sweep frequency signal generator were connected to the cathode and anode of the MFC respectively. And then adjusting amplitude was up to 20 V and the frequency was 1 Hz. After continuing 45 min and then disconnected 24 h for MFC recovery. The maximum power density after cleaning can be restored to 92.9 %–94.2%, and the impedance can be reduced by about 23 %–28.5%. It can be seen from Fig. 6c and d that the cleaning effect of external AC is more obvious, but the auxiliary equipment increase the cost and operation difficulty of MFC-based biosensor.

Although the in-situ ECS and AC enhanced cleaning can mitigate the degradation of the cathode, it is necessary to further analyze the causes of MFC performance decline and adopt more effective electrode cleaning methods to mitigate the degradation and improve the MFC long-term performance.

4. Conclusions

In this study, the UASB-MFC dual sensors system obtained good sensoring performance and treatment efficiency over a long period. Meanwhile, the potential distribution methods accelerate the re-enrichment of micro-organisms after inhibited by adverse environment, which reduced the recovery time to 55% of the original. It is found that the degradations of MFCs were mainly caused by the precipitation of Ca^{2+} and Mg^{2+} on the cathode surface. Cleaning the electrode by an self-enhanced method without external assistance ECS to mitigate the degradation of MFCs, which improve the MFCs performance to 83.2 %–84.6%. Although external AC cleaning method can give more MFCs sensors recovery, the additional instruments limited its application in some degree.

While this study focuses on the voltage recovery and electrode cleaning of MFCs in the UASB-MFC dual sensors system, the results have wider applications on other coupling process between MFC and anaerobic reactor as well as electrode recovery of MFC-based biosensors. However, more studies need to be conducted to further improve the performance of dual sensors system. Such as optimize the structure of the reactor, use of more efficient catalysts, and rapid enrichment of exoelectrogens.

Author Contributions Section

Wenbin Liu contributions to conception and design, acquisition of data, analysis and interpretation of data, Guang Yang revising the

article critically for important intellectual content; Hui Jia and Jie Wang final approval of the version to be published.

Acknowledgments

This study was financially supported by the National Natural Science Foundation of China (No.51578375), China Postdoctoral Science Foundation (2017M621081), Program for Changjiang Scholars and Innovative Research Team in University of Ministry of Education of China (Grand No. IRT-17R80). We also thanks for the support of China Scholarship Council (No.201609345007, No. 201709345009).

Appendix A. Supplementary data

Supplementary data to this article can be found online at https://doi.org/10.1016/j.chemosphere.2019.125751.

References

Bard, A.J., Faulkner, L.R., 2001. Electrochemical Methods: Fundamentals and Applications, second ed. Wiley, New York.
Chen, Z.J., Niu, Y.Y., Zhao, S., Khan, A.A., 2016. A novel biosensor for p-nitrophenol based on aerobic anode microbial fuel cell. Biosens. Bioelectron. 85, 860–868.
Chen, C.W., Lee, H.M., Chang, M.B., 2008. Inactivation of aquatic microorganisms by Low-frequency AC discharges. IEEE Trans. Plasma Sci. 36 (1), 215–219.
Cheng, S.A., Liu, H., Logan, B.E., 2006. Power densities using different cathode catalysts (Pt and CoTMPP) and polymer binders (Nafion and PTFE) in single chamber microbial fuel cells. Environ. Sci. Technol. 40 (1), 364–369.
Cheng, S.A., Xing, D.F., Logan, B.E., 2011. Electricity generation of single-chamber microbial fuel cells at low temperatures. Biosens. Bioelectron. 26 (5), 1913–1917.
Deng, Y.H., Tang, L., Zeng, G.M., Zhu, Z.J., Yan, M., 2017. Insight into highly efficient simultaneous photocatalytic removal of Cr(VI) and 2,4-diclorophenol under visible light irradiation by phosphorus doped porous ultrathin g-C3N4 nanosheets from aqueous media: performance and reaction mechanism. Appl. Catal. B Environ. 203, 343–354.
Elmekawy, A., Hegab, H.M., Pant, D., Saint, C.P., 2018. Bio-analytical applications of microbial fuel cell-based biosensors for onsite water quality monitoring. J. Appl. Microbiol. 124 (1), 302–313.
Feng, C.H., Huang, L.Q., Yu, H., Yi, X.Y., Wei, C.H., 2015. Simultaneous phenol removal, nitrification and denitrification using microbial fuel cell technology. Water Res. 76, 160–170.
Finkelstein, D.A., Tender, L.M., Zeikus, J.G., 2006. Effect of electrode potential on electrode-reducing microbiota. Environ. Sci. Technol. 40 (22), 6990–6995.
Gupta, S., Yadav, A., Verma, N., 2017. Simultaneous Cr(VI) reduction and bioelectricity generation using microbial fuel cell based on alumina-nickel nanoparticles-dispersed carbon nanofiber electrode. Chem. Eng. J. 307, 729–738.
He, Z., Mansfeld, F., 2009. Exploring the use of electrochemical impedance spectroscopy (EIS) in microbial fuel cell studies. Energy Environ. Sci. 2 (2), 215–219.
Hong, Y.Y., Call, D.F., Werner, C.M., Logan, B.E., 2011. Adaptation to high current using low external resistances eliminates power overshoot in microbial fuel cells. Biosens. Bioelectron. 28 (1), 71–76.
Hoseinzadeh, E., Rezaee, A., Farzadkia, M., 2018. Nitrate removal from pharmaceutical wastewater using microbial electrochemical system supplied through low frequency-low voltage alternating electric current. Bioelectrochemistry 120, 49–56.
Huang, X.F., Shen, C.M., Liu, J., Lu, L.J., 2015. Improved volatile fatty acid production during waste activated anaerobic fermentation by different bio-surfactants. Chem. Eng. J. 264, 280–290.
Jia, H., Yang, G., Ngo, H.H., Guo, W.S., Zhang, H.W., Gao, F., Wang, J., 2017. Enhancing simultaneous response and amplification of biosensor in microbial fuel cell-based upflow anaerobic sludge bed reactor supplemented with zero-valent iron. Chem. Eng. J. 327, 1117–1127.
Jia, H., Liu, W.B., Wang, J., Ngo, H.H., Zhang, H.W., 2018. Optimization of sensing performance in an integrated dual sensors system combining microbial fuel cells and upflow anaerobic sludge bed reactor. Chemosphere 210, 931–940.
Jiang, J., Gong, C., Wang, J., Tian, S., Zhang, Y., 2014. Effects of ultrasound pretreatment on the amount of dissolved organic matter extracted from food waste. Bioresour. Technol. 155, 266–271.
Jiang, Y., Liang, P., Huang, X., Ren, Z.Y., 2018. A novel microbial fuel cell sensor with a gas diffusion biocathode sensing element for water and air quality monitoring. Chemosphere 203, 21–25.
Jiang, Y., Liang, P., Liu, P.P., Wang, D.L., Miao, B., Huang, X., 2017. A novel microbial fuel cell sensor with biocathode sensor element. Biosens. Bioelectron. 94, 344–350.
Kang, X.H., Sun, Y.M., Li, L.H., Kong, X.Y., Yuan, Z.H., 2018. Improving methane production from anaerobic digestion of pennisetum hybrid by alkaline pretreatment. Bioresour. Technol. 255, 205–212.
Kaur, A., Kim, J.R., Michie, I., Dinsdale, R.M., Guwy, A.J., 2013. Microbial fuel cell type biosensor for specific volatile fatty acids using acclimated bacterial communities. Biosens. Bioelectron. 47, 50–55.
Kaur, A., Ibrahim, S., Pickett, C.J., Michie, I.S., Dinsdale, R.M., Guwy, A.J., Premier, G.C., 2014. Anode modification to improve the performance of a microbial fuel cell volatile fatty acid biosensor. Sensor Actuat B-chem. 201, 266–273.
Kim, K.Y., Yang, E., Logan, B.E., 2015. Impact of electrode configurations on retention time and domestic wastewater treatment efficiency using microbial fuel cells. Water Res. 80, 41–46.
Lee, W.S., Chua, A.S.M., Yeoh, H.K., Ngoh, G.C., 2014. A review of the production and applications of waste-derived volatile fatty acids. Chem. Eng. J. 235, 83–99.
Li, Y., Yang, H.Y., Shen, J.Y., Mu, Y., 2016. Enhancement of azo dye decolourization in a MFC-MEC coupled system. Bioresour. Technol. 202, 93–100.
Liao, Q., Zhang, J., Li, J., Ye, D.D., Zhu, X., Zhang, B., 2015. Increased performance of a tubular microbial fuel cell with a rotating carbon-brush anode. Biosens. Bioelectron. 63, 558–562.
Liu, H., Logan, B.E., 2004. Electricity generation using an air-cathode single chamber microbial fuel cell in the presence and absence of a proton exchange membrane. Environ. Sci. Technol. 38, 4040–4046.
Liu, W.B., Jia, H., Wang, J., 2018. Microbial fuel cell and membrane bioreactor coupling system: recent trends. Environ Sci Pollut 25 (24), 23631–23644.
Logan, B.E., Hamelers, B., Rozendal, R.A., Schroeder, U., Keller, J., Freguia, S., 2006. Microbial fuel cells: methodology and technology. Environ. Sci. Technol. 40 (17), 5181–5192.
Miao, H., Lu, M., Zhao, M., Huang, Z., Ren, H., Yan, Q., Ruan, W., 2013. Enhancement of Taihu blue algae anaerobic digestion efficiency by natural storage. Bioresour. Technol. 149, 359–366.
Miller, D.J., Araujo, P.A., Correia, P.B., Ramsey, M.M., Kruithof, J.C., 2012. Short-term anhersion and long-term biofouling testing of polydopamine and poly (ethylene glycol) surface modifications of membranes and feed spacers for biofouling control. Water Res. 46 (12), 3737–3753.
Paitiera, A., Godaina, A., Delina Lyona, D., Haddoura, N., Monierb, J.K., 2017. Microbial fuel cell anodic microbial population dynamics during MFC startup. Biosens. Bioelectron. 92, 357–363.
Palaniappan, S., Subramaniam, P., Palaniappan, S., Murugesan, S., Tamilselvi, M., Sivakumar, L., 2019. Bioremediation of wastewater through a quorum sensing triggered MFC: a sustainable measure for waste to energy concept. J. Environ. Manag. 237, 84–93.
Pandey, P., Shinde, V.N., Deopurkar, R.L., Kale, S.P., 2016. Recent advances in the use of different substrates in microbial fuel cells toward wastewater treatment and simultaneous energy recovery. Appl. Energy 168, 706–723.
Ray, S.G., Ghangrekar, M.M., 2015. Enhancing organic matter removal, biopolymer recovery and electricity generation from distillery wastewater by combining fungal fermentation and microbial fuel cell. Bioresour. Technol. 176, 8–14.
Rebecchi, S., Pinelli, D., Bertin, L., Zama, F., Fava, F., Frascari, D., 2016. Volatile fatty acids recovery from the effluent of an acidogenic digestion process fed with grape pomace by adsorption on ion exchange resins. Chem. Eng. J. 306, 629–639.
Ren, Z., Yan, H., Wang, W., Mench, M.M., 2011. Characterization of microbial fuel cells at microbially and electro-chemically meaningful timescales. Environ. Sci. Technol. 45 (6), 2435–2441.
Soon, B.Q., Liang, C., Ralf, C.R., 2015. In-line deoxygenation for organic carbon detections in seawater using a marine microbial fuel cell-biosensor. Bioresour. Technol. 182, 34–40.
Stein, N.E., Keesman, K.J., Hamelers, H.V.M., van Straten, G., 2011. Kinetic models for detection of toxicity in a microbial fuel cell based biosensor. Biosens. Bioelectron. 26, 3115–3120.
Tejedor-Sanz, S., Ortiz, J.M., Esteve-Nunez, A., 2017. Merging microbial electrochemical systems with electrocoagulation pretreatment for achieving a complete treatment of brewery wastewater. Chem. Eng. J. 330, 1068–1074.
Tian, Y., Li, H., Li, L.P., Sun, X.Y., 2015. In-situ integration of microbial fuel cell with hollow-fiber membrane bioreactor for wastewater treatment and membrane fouling mitigation. Biosens. Bioelectron. 64, 189–195.
Velasquez-Orta, S.B., Werner, D., Varia, J.C., Mgana, S., 2017. Microbial fuel cells for inexpensive continuous in-suit monitoring of groundwater quality. Water Res. 117, 9–17.
Wagner, A.O., Reitschuler, C., Illmer, P., 2014. Effect of different acetate: propionate ratios on the methanogenic community during thermophilic anaerobic digestion in batch experiments. Biochem. Eng. J. 90, 154–161.
Wang, C.L., Yao, Z.B., Bai, L.L., Wang, C.H., 2019. Application of a microbial fuel cell-based biosensor for the energy-saving operation of macrophyte residues bioreactor with low concentration of dissolved organic carbon in effluents. Chemosphere 220, 1075–1082.
Wang, X., Feng, Y.J., Ren, N.Q., Wang, H.M., Lee, H., Li, N., 2009. Accelerated start-up of two-chambered microbial fuel cells: effect of anodic positive poised potential. Electrochim. Acta 54 (3), 1109–1114.
Wang, Y.F., Hui, J., Wang, J., 2018. Impacts of energy distribution and electric field on membrane fouling control in microbial fuel cell-membrane bioreactor (MFC-MBR) coupling system. Bioresour. Technol. 269, 339–345.
Wu, S., Li, H., Zhou, X., Liang, P., Zhang, X., 2016. A novel pilot-scale stacked microbial fuel cell for efficient electricity generation and wastewater treatment. Water Res. 98, 396–403.
Yang, H.J., Zhou, M.H., Liu, M.M., 2015. Microbial fuel cells for biosensor applications. Biotechnol. Lett. 37 (12), 2357–2364.

Yang, G., Wang, J., Zhang, H.W., Hui, J., 2019. Applying bio-electric field of microbial fuel cell-upflow anaerobic sludge blanket reactor catalyzed blast furnace dusting ash for promoting anaerobic digestion. Water Res. 149, 215–224.
Zeng, L.B., Li, X.Y., Shi, Y.R., Qi, Y.F., Huang, D.Q., 2017. FePO4 based single chamber air-cathode microbial fuel cell for online monitoring levofloxacin. Biosens. Bioelectron. 91, 367–373.
Zhang, M.M., Wang, Y., Liang, P., Zhao, X., 2019. Combined photoelectrocatalytic microbial fuel cell (PEC-MFC) degradation of refractory organic pollutants and in-situ electricity utilization. Combined photo-electrocatalytic microbial fuel cell (PEC-MFC) degradation of refractory organic pollutants and in-situ electricity utilization. Chemosphere 214, 669–678.
Zhang, W.L., Zhang, L., Li, A.M., 2015. Anaerobic co-digestion of food waste with MSW incineration plant fresh leachate: process performance and synergistic effects. Chem. Eng. J. 259, 795–805.
Zhang, X., Cheng, S., Huang, X., Logan, B.E., 2010. Improved performance of single-chamber microbial fuel cells through control of membrane deformation. Biosens. Bioelectron. 25 (7), 1825–1828.
Zhao, H.H., Kong, C.H., 2018. Enhanced removal of p-nitrophenol in a microbial fuel cell after long-term operation and the catabolic versatility of its microbial community. Chem. Eng. J. 339, 424–431.
Zhou, L., Yan, X., Yan, Y., Li, T., An, J., Liao, C., Li, N., Wang, X., 2020. Electrode potential regulates phenol degradation pathways in oxygen-diffused microbial electrochemical system. Chem. Eng. J. 381, 122663.